COMSOL CONFERENCE BOSTON 2012

ADVANCEMENTS IN CARBON DIOXIDE AND WATER VAPOR SEPARATIONS USING COMSOL

James C. Knox, Kenneth Kittredge, Robert F. Coker, Ramona Cummings, and Carlos F. Gomez

NASA Marshall Space Flight Center, Huntsville, Alabama, 35812, USA

COMSOL Conference Boston 2012

Introduction

- NASA's Advanced Exploration Systems Program …

  … is pioneering new approaches for rapidly developing prototype systems, demonstrating key capabilities, and validating operational concepts for future human missions beyond Earth orbit.

- The Atmosphere Resource Recovery and Environmental Monitoring Project …

  … main objectives are to mature integrated AR and environmental monitoring (EM) subsystems derived directly from the ISS AR subsystem architecture

  … reduce developmental and mission risk, improve reliability, lower lifecycle costs, and demonstrate operational process design and system architectural concepts for future human missions beyond Earth orbit.

http://www.nasa.gov/directorates/heo/aes/index.html

Perry, J. L., Abney, M. B., Knox, J. C., Parrish, K. J., Roman, M. C., and Jan, D. L. "Integrated Atmosphere Resource Recovery and Environmental Monitoring Technology Demonstration for Deep Space Exploration," International Conference on Environmental Systems. AIAA, San Diego, 2012.

Approach - CO_2 Removal, Bulk Drying, and Residual Drying

1. Characterize candidate sorbents and compare directly with state-of-the-art sorbents. Select promising sorbent candidates for life support process of interest.
2. Develop new or modify existing mathematical models and computer simulations for process of interest.
3. Via simulation, optimize cyclic test configuration (e.g., canister design and cycle parameters).
4. Fabricate test article and execute test series. Evaluate sorbent efficacy for go/no go to next larger scale. Validate and refine simulation.
5. For promising sorbents, repeat steps 3 and 4 while increasing scale until full-scale for the process of interest is attained.
6. Incorporate the full-scale system into the integrated Atmosphere Revitalization test configuration and evaluate via integrated testing.
7. Provide technology solution to spacecraft flight system developer.

1-D Model Equations

Gas Phase Mass Balance

$$\frac{\partial c}{\partial t}+\left(\frac{1-\varepsilon}{\varepsilon}\right)\frac{\partial \overline{q}}{\partial t}-D_L\frac{\partial^2 c}{\partial x^2}=-\upsilon_i\frac{\partial c}{\partial x} \quad (1)$$

Gas Phase B.C.

$$-D_L\left.\frac{\partial c}{\partial x}\right|_{x=0}=\upsilon_i(c_o-c) \qquad \left.\frac{\partial c}{\partial x}\right|_{x=L}=0 \quad (2)$$

Sorbent Mass Balance

$$\frac{\partial \overline{q}}{\partial t}=k_m(q^*-\overline{q}) \quad (3)$$

Heat Balance

$$\varepsilon a_f\rho_g c_{pg}\frac{\partial T_g}{\partial t}-\varepsilon a_f k_g\frac{\partial^2 T_g}{\partial x^2}=-\varepsilon a_f\rho_g\upsilon_i c_{pg}\frac{\partial T_g}{\partial x}+a_s h_{sg}\left(T_s-T_g\right)+\varepsilon_w P_i h_{wg}\left(T_w-T_g\right) \quad (4)$$

Heat Balance B.C.

$$-k_g\left.\frac{\partial T_g}{\partial x}\right|_{x=0}=-\rho_g\upsilon_i c_{pg}\left(T_0-T_g\right) \qquad \left.\frac{\partial T_g}{\partial x}\right|_{x=L}=0 \quad (5)$$

Sorbent Heat Balance

$$a_f\rho_s c_{ps}\frac{\partial T_s}{\partial t}-a_f k_s\frac{\partial^2 T_s}{\partial x^2}=a_s h_{sg}\left(T_g-T_s\right)-a_f\partial H\frac{\partial q}{\partial t} \quad (6)$$

Column Heat Balance

$$a_w\rho_w c_{pw}\frac{\partial T_w}{\partial t}-a_w k_w\frac{\partial^2 T_w}{\partial x^2}=\varepsilon_w P_i h_{wg}\left(T_g-T_w\right)+P_o h_{wa}\left(T_a-T_w\right) \quad (7)$$

Toth Isotherm

$$n=\frac{ap}{\left[1+(bp)^t\right]^{1/t}}; \qquad b=b_0\exp(E/T); \qquad a=a_0\exp(E/T); \qquad t=t_0+c/T \quad (8)$$

Axial Dispersion Coefficient

$$\frac{1}{Pe_2}=\frac{0.73\varepsilon}{\mathrm{Re}\,Sc}+\frac{1}{2\left(1+\dfrac{13\cdot 0.73\varepsilon}{\mathrm{Re}\,Sc}\right)} \qquad 0.0377<2R_p<0.607 \text{ cm} \quad (9)$$

Breakthrough Test Apparatus

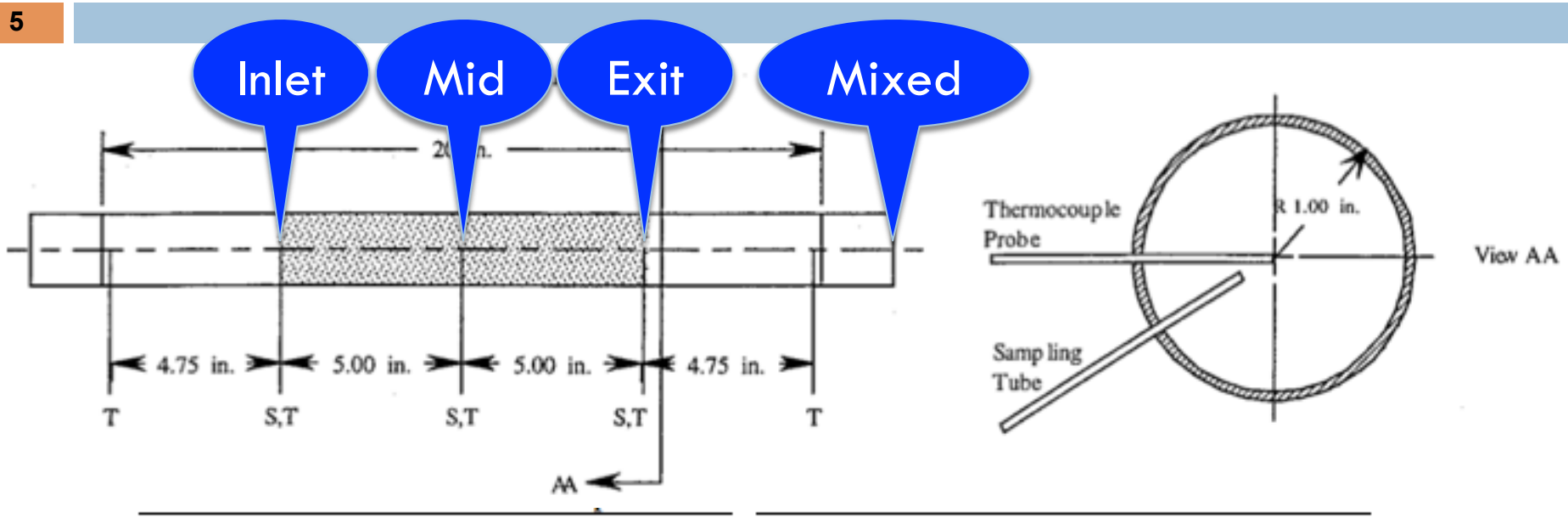

Adsorbent		Fixed-bed	
Pellet radius	$R_p = 1.02$ mm	Bed height	$L = 0.254$ m
Particle density	$\rho_s = 1180$ kg m^{-3}	Bed mass	$m = 396$ g
Skeletal density	$\rho_{sk} = 2040$ kg m^{-3}	Bed internal diameter	$R_i = 47.6$ mm
Heat capacity	$c_{ps} = 920$ J kg^{-1} K^{-1}	Column wall thickness	$l = 1.59$ mm
Langmuir surface area	$A_L = 463$ m^2 g^{-1}	Wall heat capacity	$c_{pw} = 475$ J kg^{-1} K^{-1}
		Wall density	$\rho_w = 7833$ kg m^{-3}

1-D Results – Carbon Dioxide on Zeolite CaA (5A)

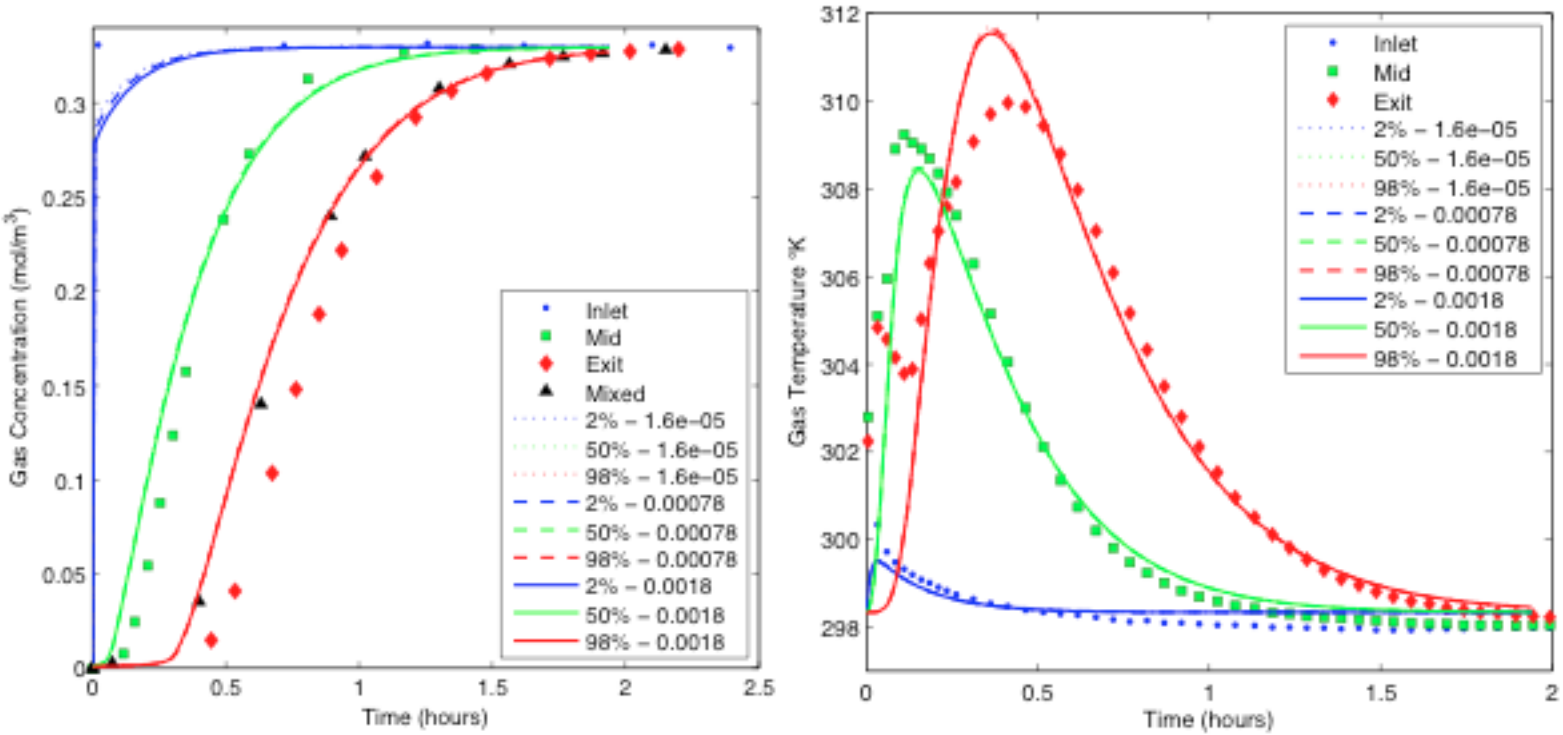

Figure 2. Breakthrough test data and 1-D simulation results for CO_2 on zeolite CaA. *Concentration history (left) and temperature history (right). Experimental data are shown as symbols. Simulation data at the inlet (2%), midpoint (50%), and exit (98%) are shown as lines. Three values for axial dispersion (units are $m^2\ s^{-1}$) are compared in these figures, however, their influence is negligible on simulation results.*

1-D Results – Water on CaA

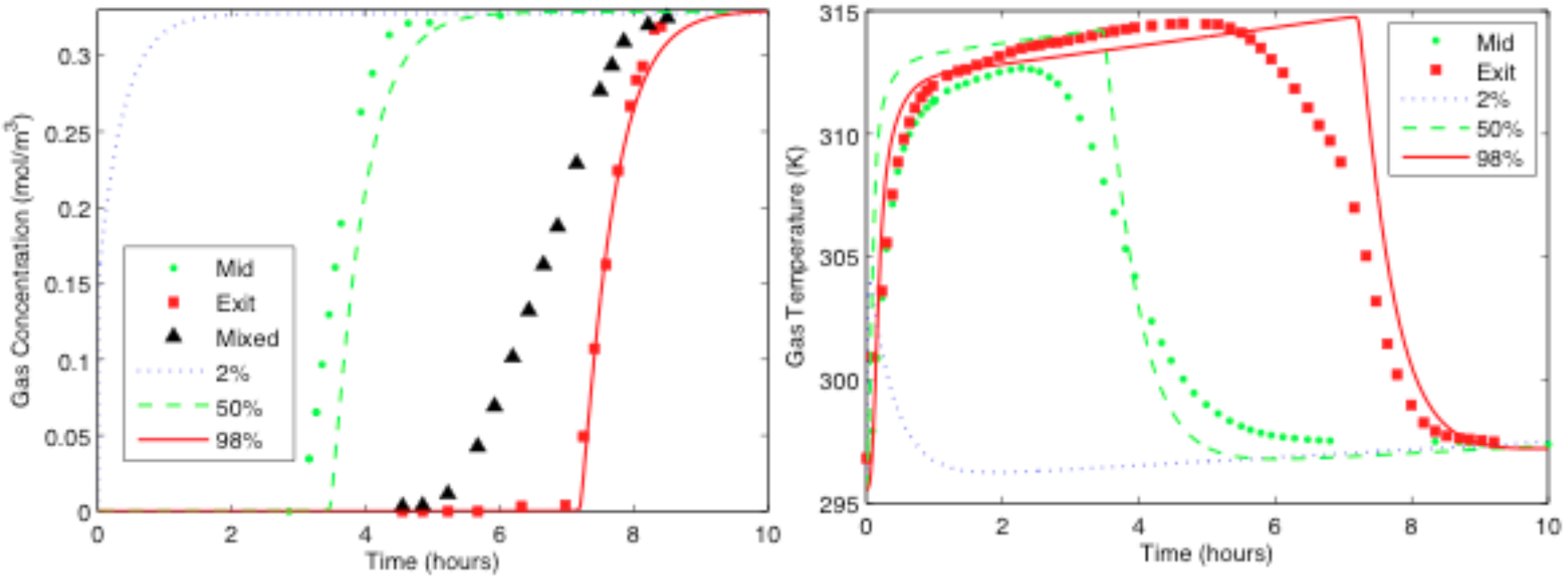

Figure 3. Breakthrough test data and 1-D simulation results for H_2O on zeolite CaA. *Concentration history (left) and temperature history (right). Experimental data are shown as symbols. Simulation data at the inlet (2%), midpoint (50%), and exit (98%) are shown as lines.*

2-D Model Equations

- Free and Porous Media Flow, including Darcy and Forchheimer terms (Eq. (10))

$$\frac{\rho_g}{\varepsilon}\left(\frac{\partial \vec{u}_i}{\partial t}+(\vec{u}_i\cdot\nabla)\frac{\vec{u}_i}{\varepsilon}\right)=\nabla\cdot\left[-pI+\frac{\mu}{\varepsilon}(\nabla\vec{u}_i+\nabla\vec{u}_i)^T-\frac{2\mu}{3\varepsilon}(\nabla\cdot\vec{u}_i)I\right]-\left(\frac{\mu}{\kappa}+\beta_F|u_i|\right)\vec{u}_i$$

$$\frac{\partial(\varepsilon\rho_g)}{\partial t}+\nabla\cdot(\rho_g\vec{u}_i)=0 \qquad (10)$$

- Transport of Diluted Species (Eq. (11))

$$\frac{\partial c}{\partial t}+\nabla\cdot\vec{N}=R_i$$

$$\vec{N}=-D_L\nabla c+\vec{u}_i c \qquad (11)$$

- Distributed ODEs and DAEs (adsorbent mass balance; same as Eq. (3))
- Heat Transfer (Eq. (12))

$$(\rho C_p)_{EQ}\frac{\partial T_g}{\partial t}+\rho_g c_{pg}\vec{u}_i\cdot\nabla T_g=\nabla\cdot(k_{EQ}\nabla T_g)+Q \qquad (12a)$$

$$(\rho C_p)_{EQ}=(1-\varepsilon)\rho_s c_{ps}+\varepsilon\rho_g c_{pg} \qquad (12b)$$

$$k_{EQ}=(1-\varepsilon)k_s+\varepsilon k_g \qquad (12c)$$

Porosity variation is accounted for in Eq. (13), where y is the distance to the wall [6]

$$\varepsilon=\varepsilon_\infty\left[1+C\exp\left(-N\frac{y}{d_p}\right)\right]\text{ with } N=2\ldots8 \text{ and } C=\frac{1}{\varepsilon_\infty-1} \qquad (13)$$

2-D Model Results – Porosity Variation Near Wall

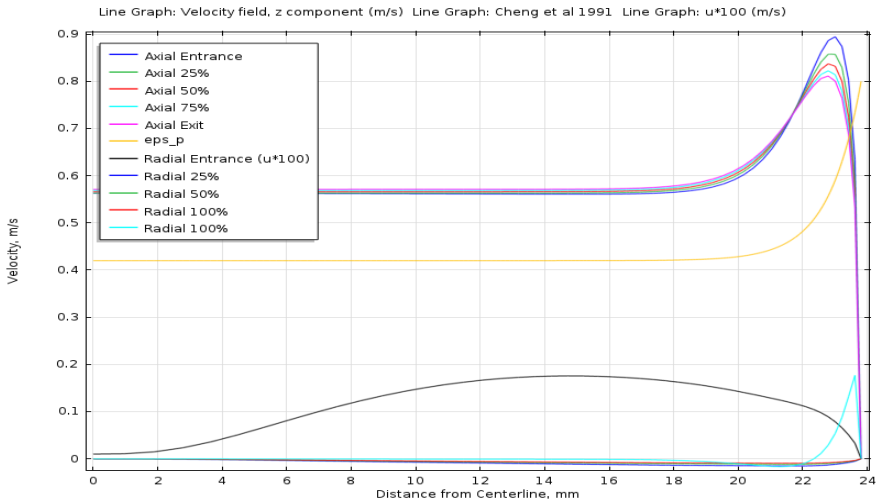

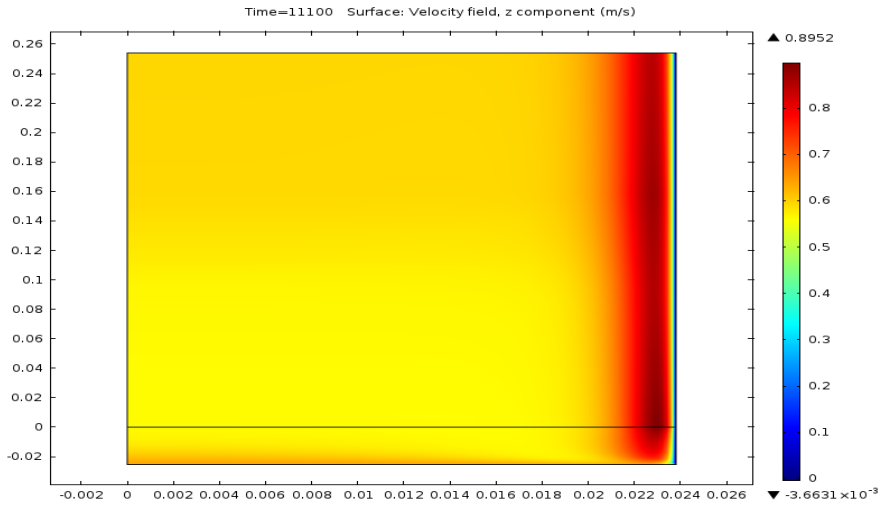

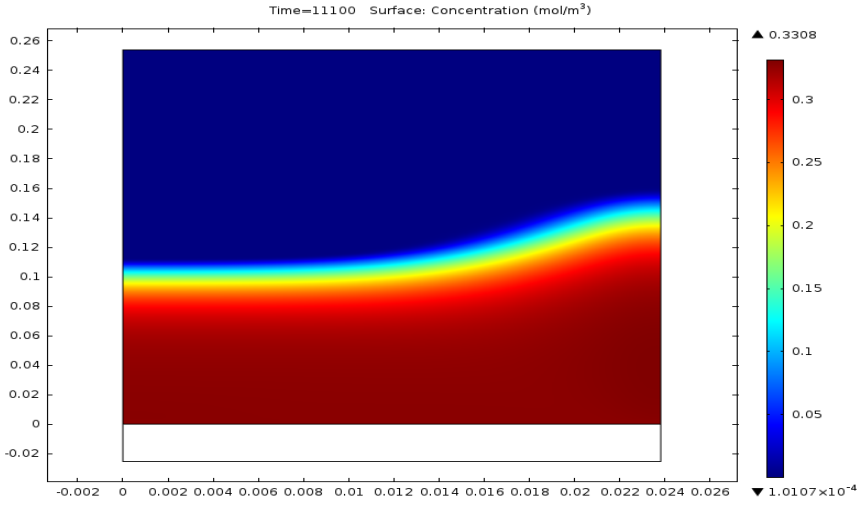

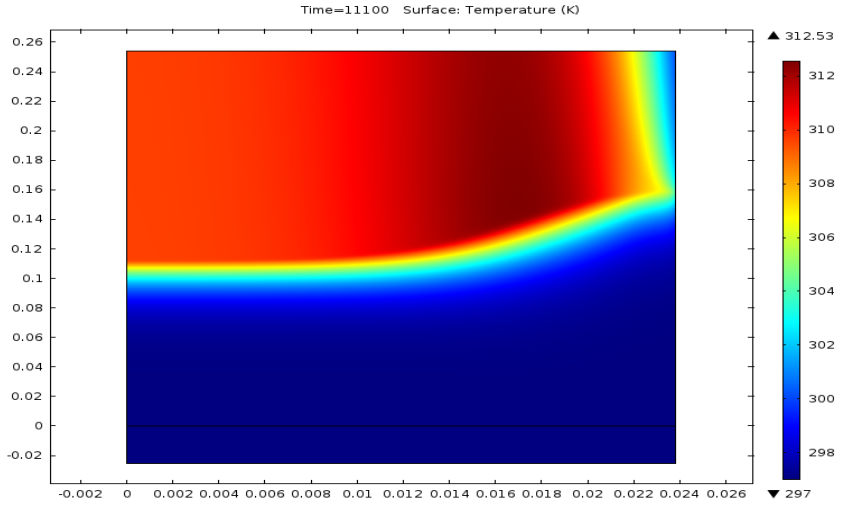

2-D Model Results – Carbon Dioxide on CaA

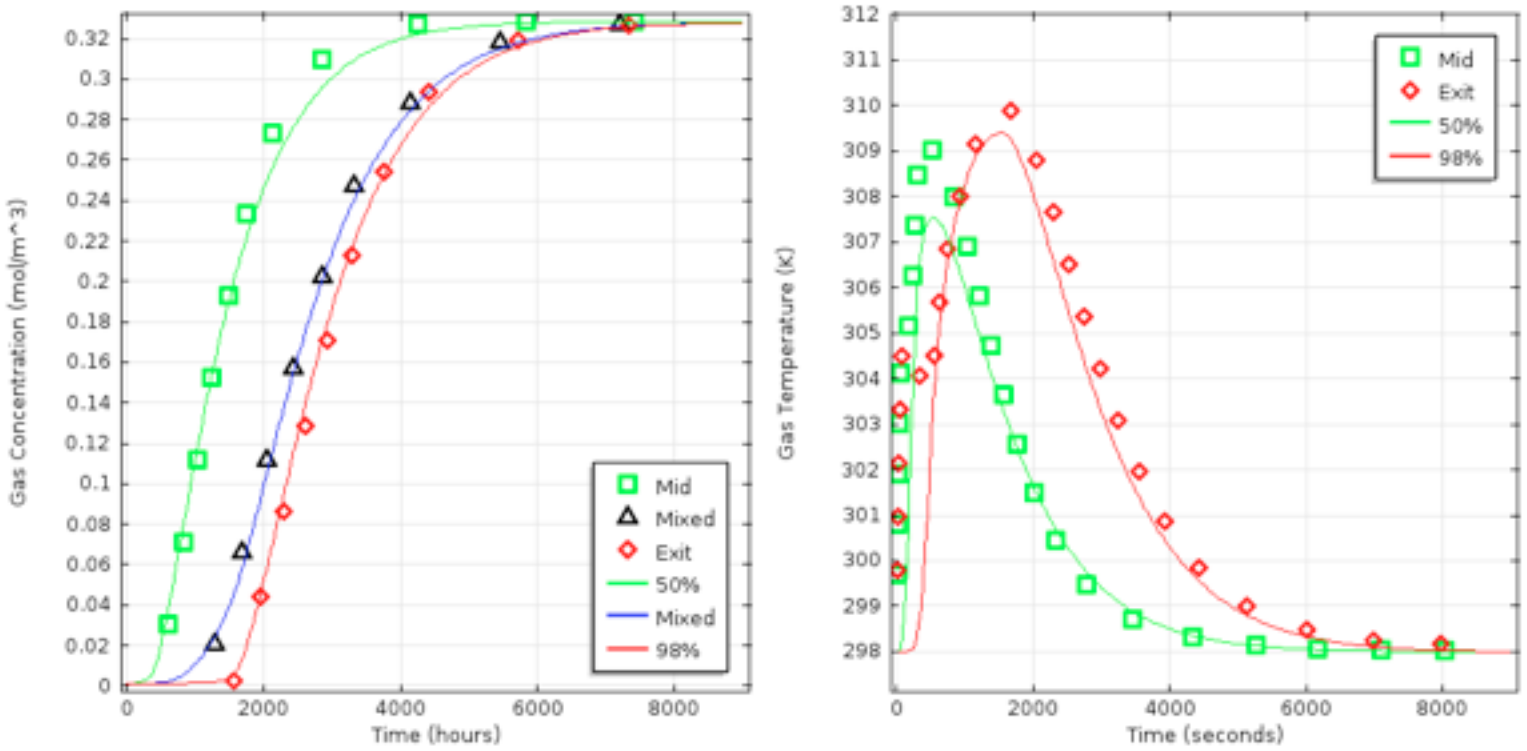

Figure 4. Breakthrough test data and 2-D axisymmetric simulation results for CO_2 on zeolite CaA.

2-D Model Results – Water Vapor on CaA

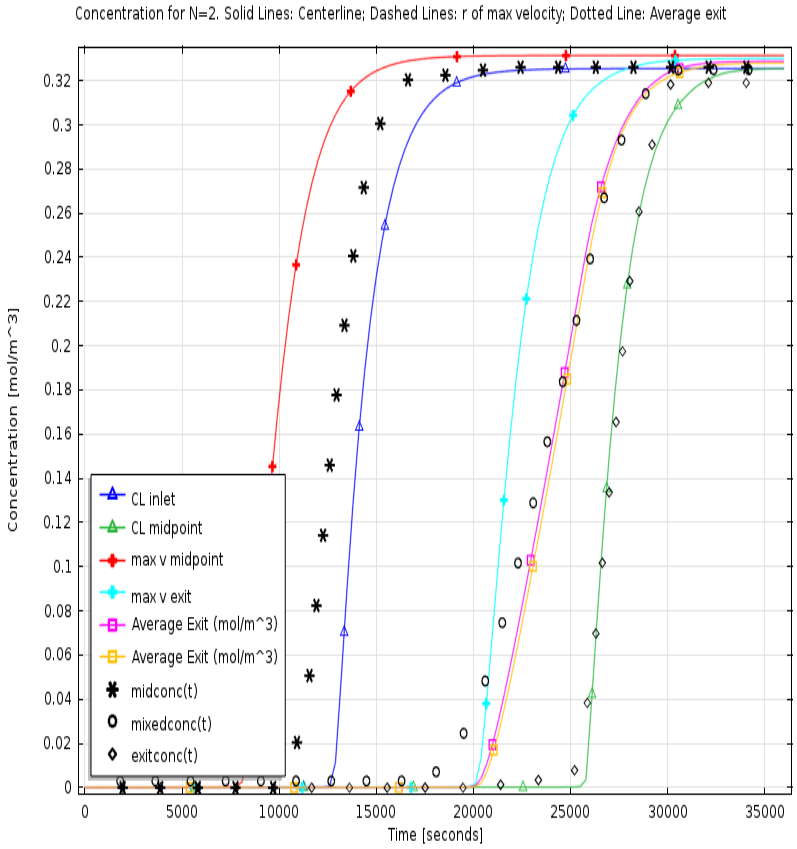

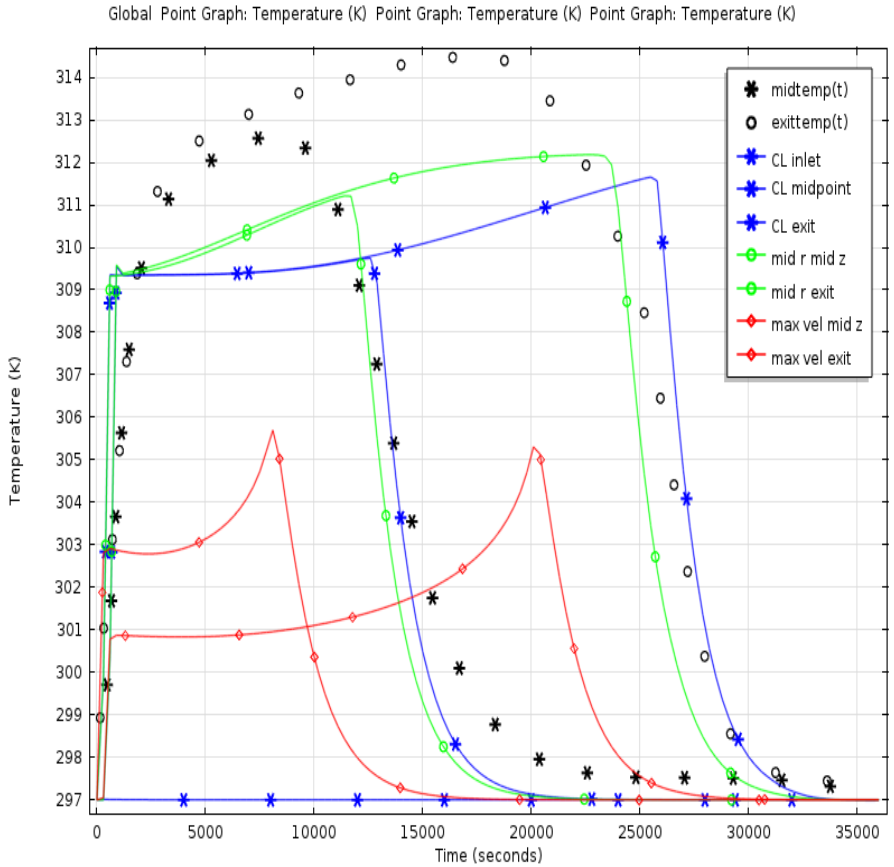

Isothermal Bulk Desiccant – Subscale Test Article

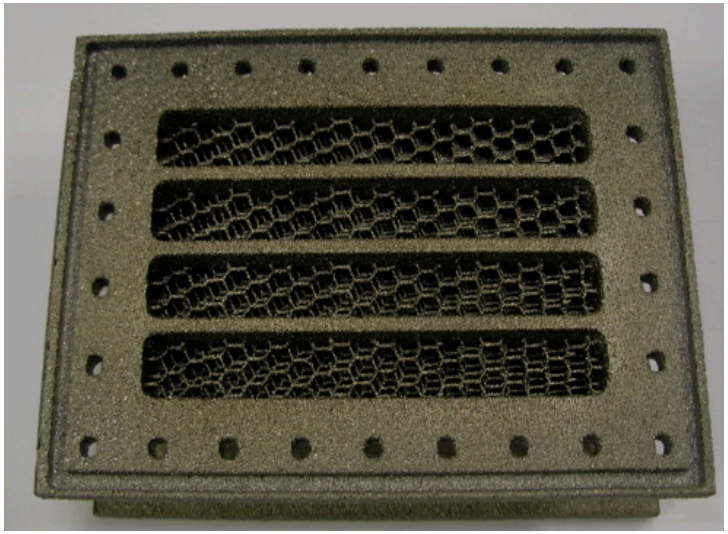

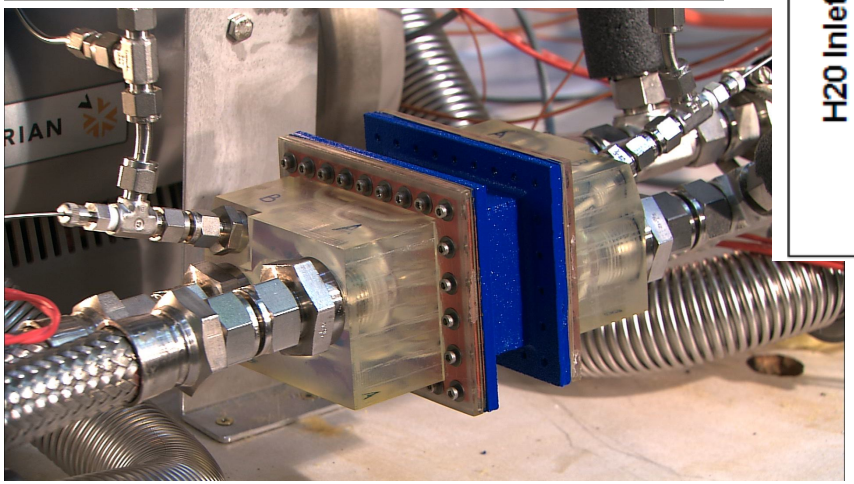

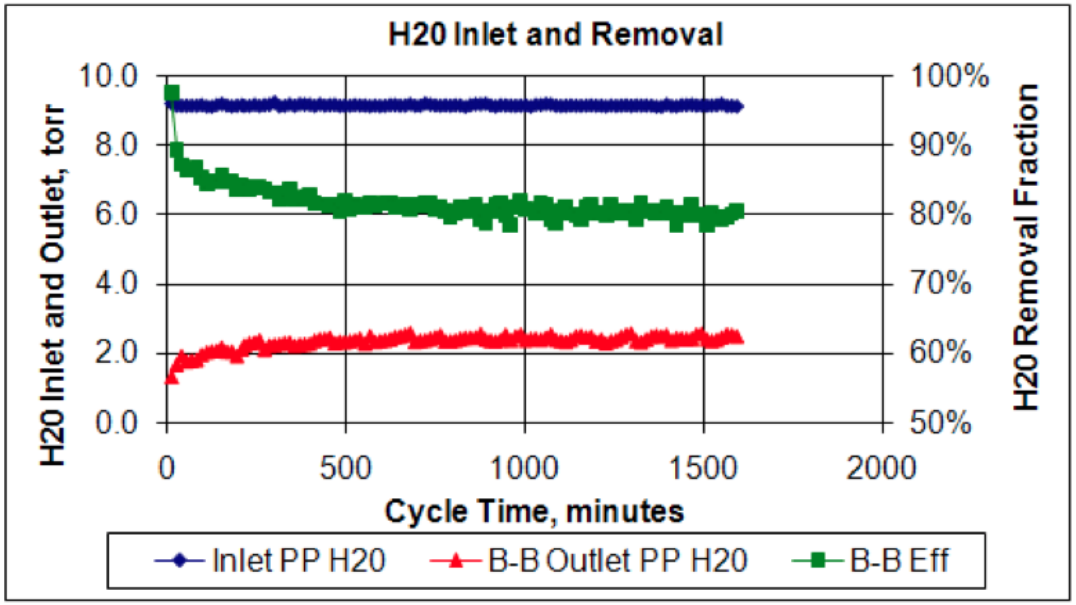

Perry, J., Howard, D. F., Knox, J. C., and Junaedi, C. "Engineered Structured Sorbents for the Adsorption of Carbon Dioxide and Water Vapor from Manned Spacecraft Atmospheres: Applications and Testing 2008/2009," International Conference On Environmental Systems. SAE, Savannah, GA, 2009.

Isothermal Bulk Desiccant – 3-D Model

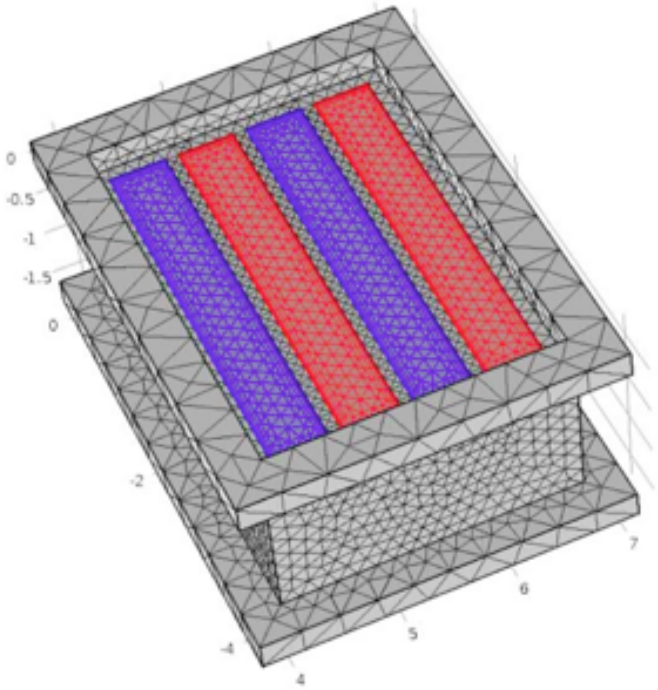

Figure 16. Meshed IBD 4-column model. *The red and blue regions are paired wet/dry inlets/exits of the columns. The size of the IBD bed in the three dimensions are shown in inches.*

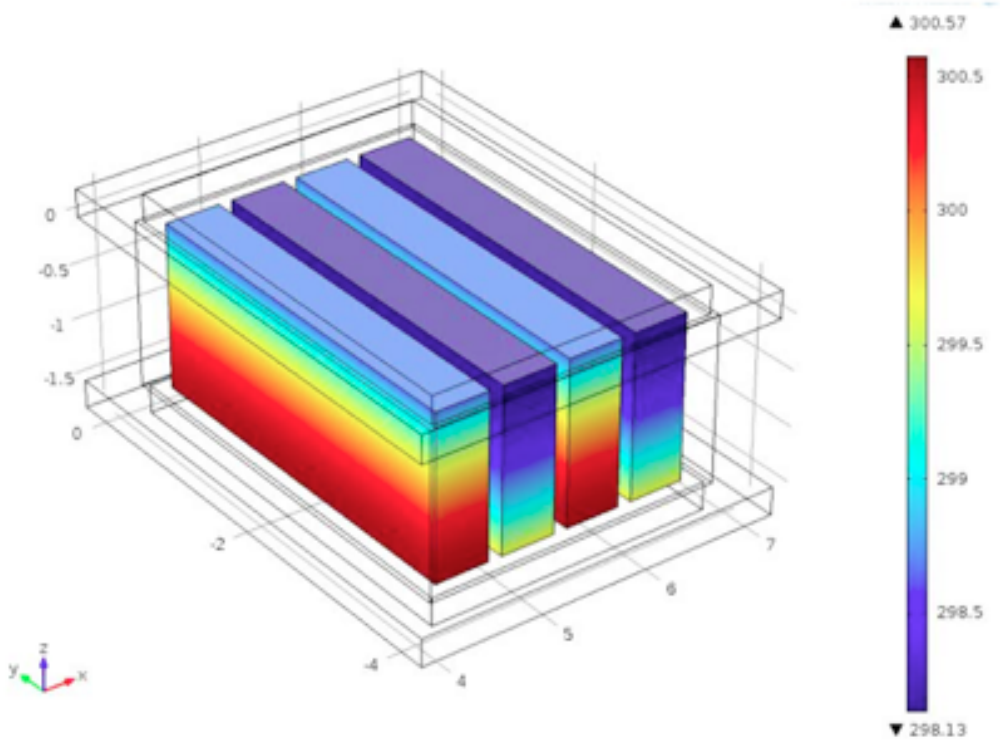

Figure 20. Temperatures (in K) on the bed surfaces at the end of the simulation. *Counting from left to right, columns 1 and 3 have wet air flowing downward and columns 2 and 4 have dry air flowing upward.*

Isothermal Bulk Desiccant – 3-D Model Results

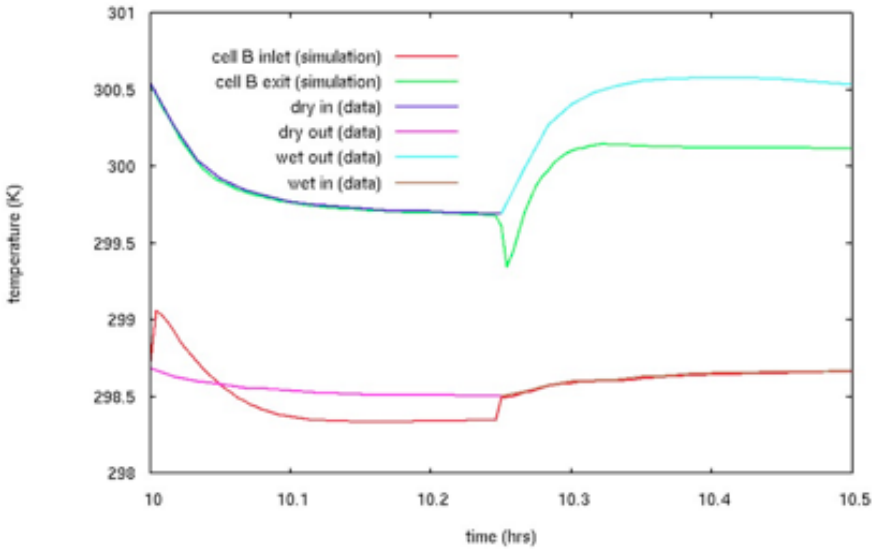

Figure 17. Temperature comparison. *The 'in' data (upper left and bottom right curves) are used as boundary conditions in the simulation. The values were taken at the center-line of the left red bed in Fig. 17, on the inlet and exit surfaces. Note the inlet and exit of cell B are spatially fixed, so that the 'inlet' is where wet air enters, but dry air exits.*

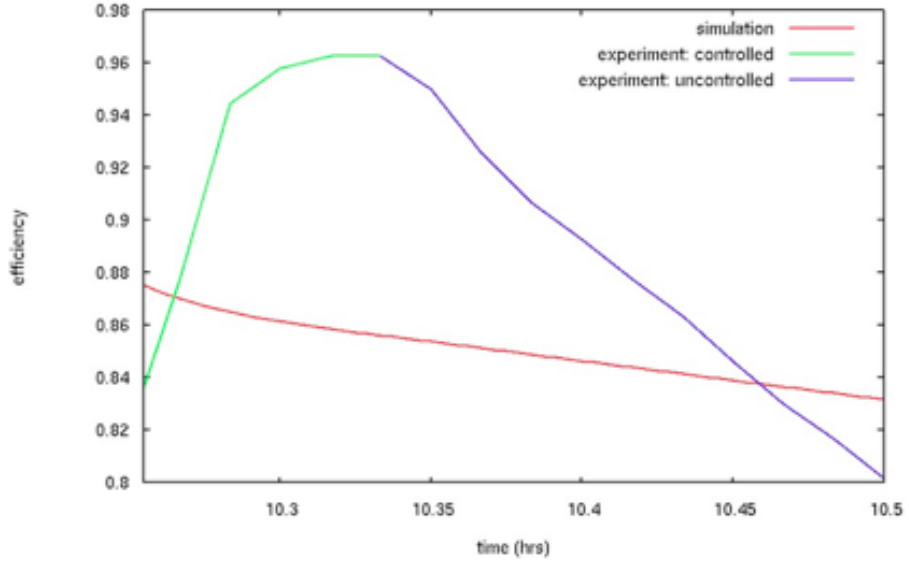

Figure 19. Efficiency, η, of the simulation compared to experiment over the last half-cycle. *During the 'controlled' period of each half-cycle, the dew point measuring device is calibrating, so the resulting concentration and partial pressures are uncertain.*

Microlith® Residual Humidity Sorbent Design

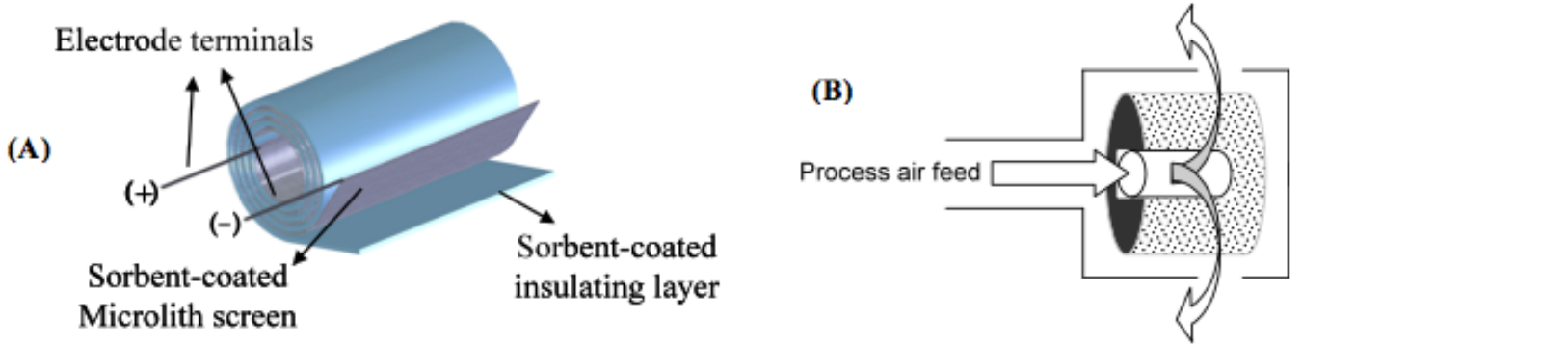

Figure 3. A simplified Microlith-based radial flow adsorber design consisting of a "jelly-roll" coil of sorbent-coated Microlith screens and sorbent-coated insulating meshes (A) in a radial flow configuration (B).

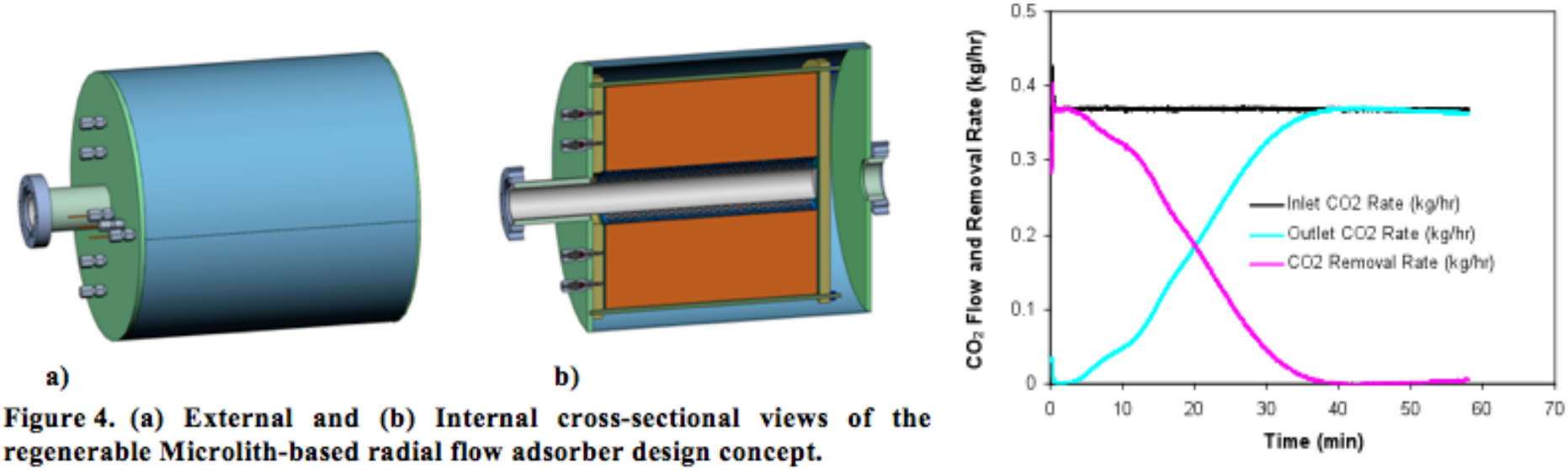

Figure 4. (a) External and (b) Internal cross-sectional views of the regenerable Microlith-based radial flow adsorber design concept.

Junaedi , C. et. al., "Compact, Lightweight Adsorber and Sabatier Reactor for CO2 Capture and Reduction for Consumable and Propellant Production," International Conference on Environmental Systems. AIAA, San Diego, 2012.

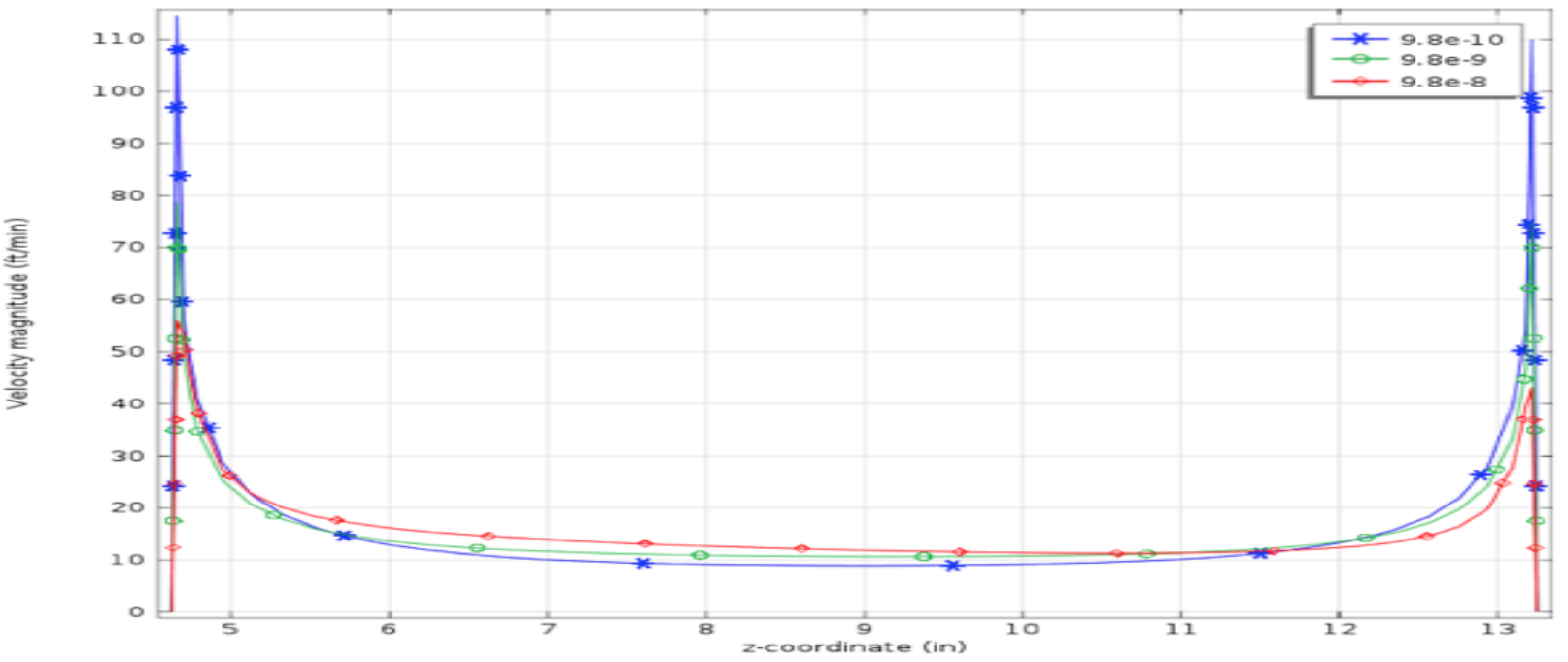

Figure 22. Jelly Roll Exit Velocities

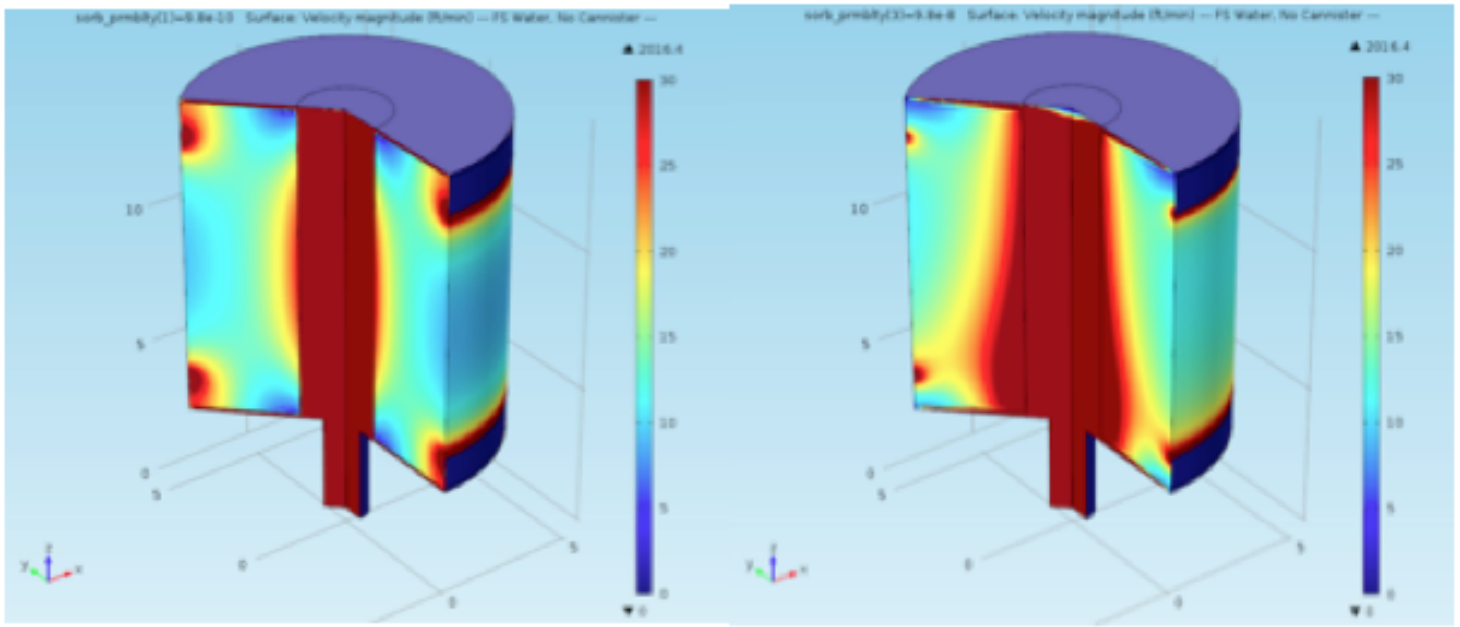

Figure 23. 3-D Velocity Mapping of the Jelly Roll for the Lowest (left) and Highest (right) Permeability Values

Linear Microlith: Velocity Results

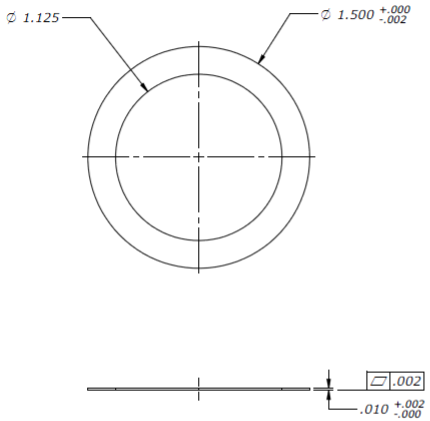

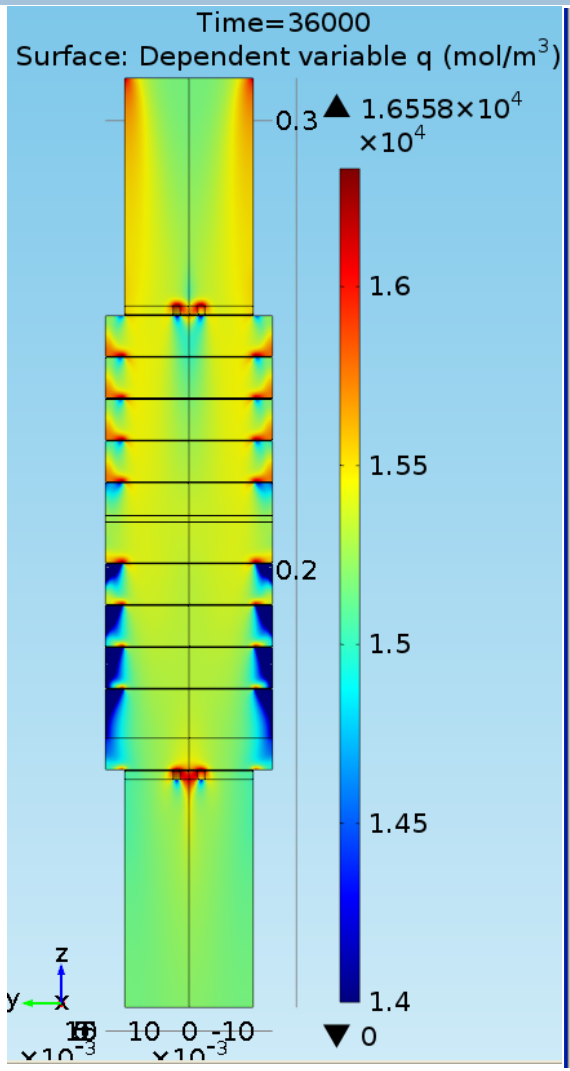

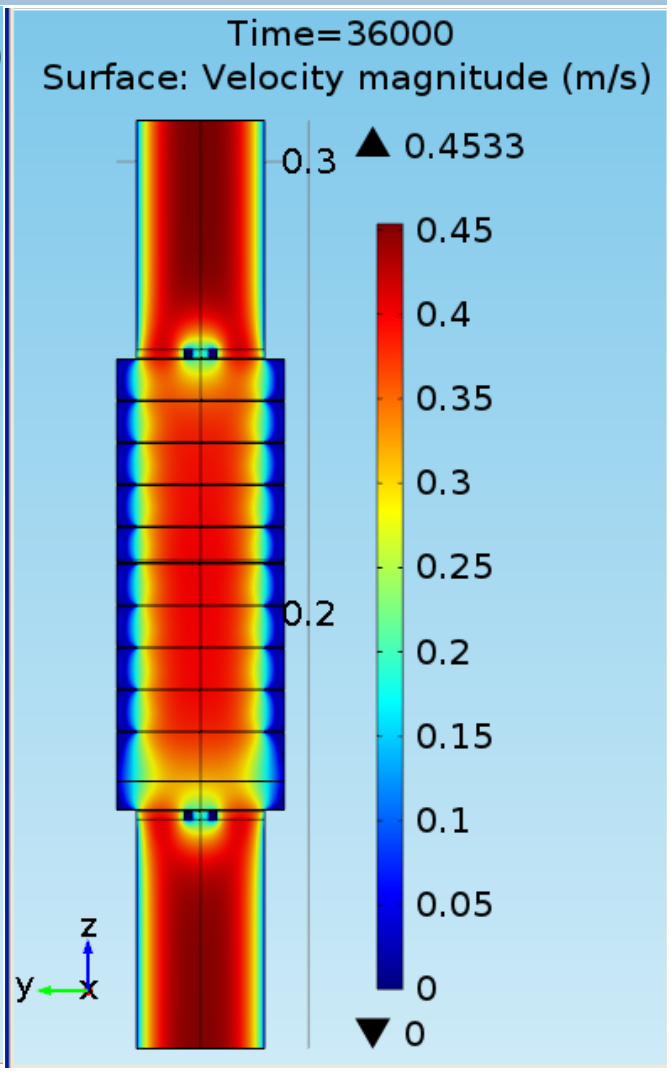

Packed Bed Vacuum Desorption

Bed Loading CO_2

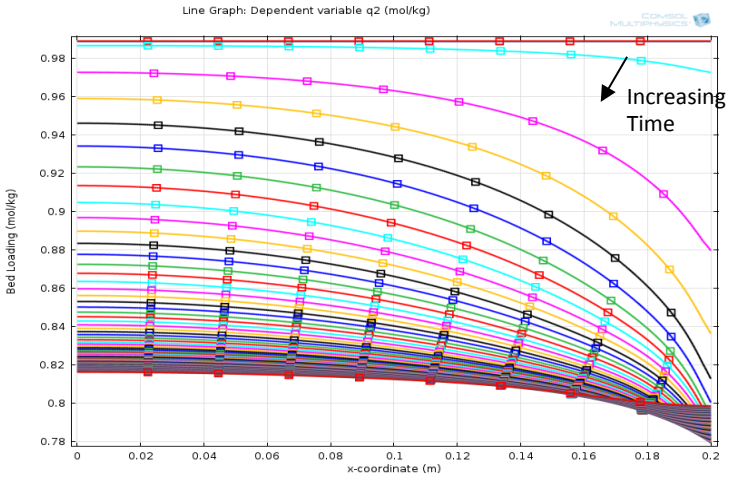

Temperature

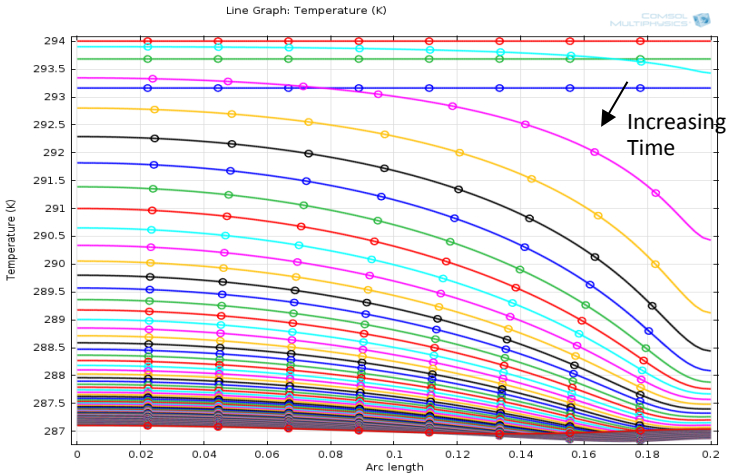

Exit Mass Fraction

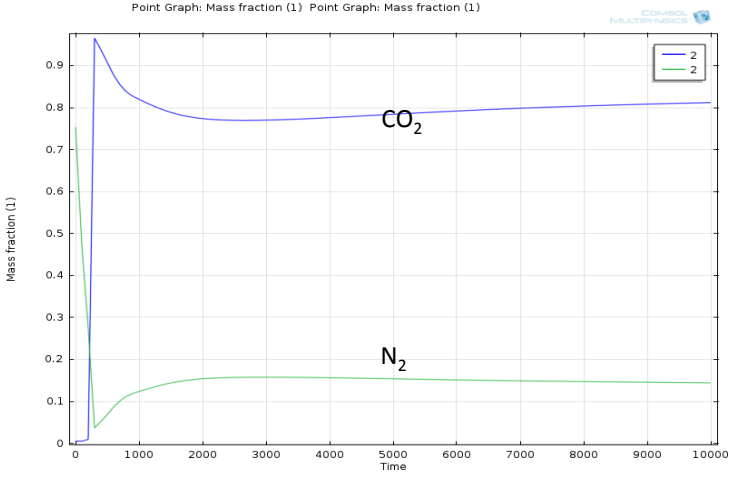

Closed End Mass Fraction

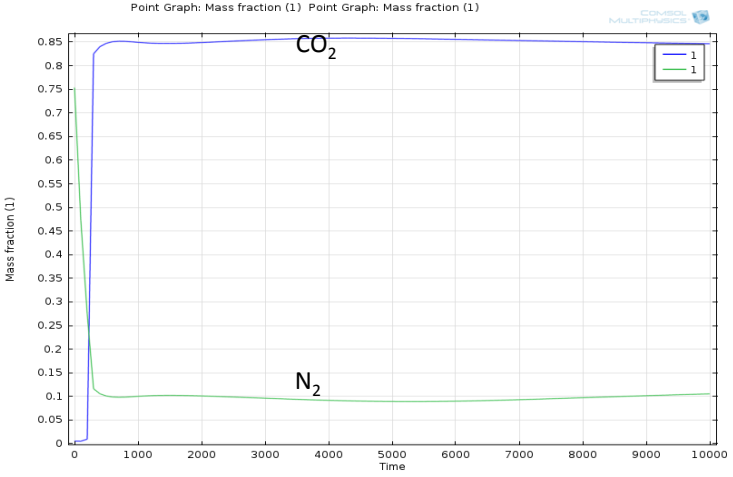

Conclusions

- Flat NASA budgets suggest innovative approaches to sorption system development
- For AES ARREM CO_2 Removal, testing is being supplemented with multi-dimensional modeling and simulation to reduce costs and optimize hardware designs
  - Empirical determination of mass transfer coefficients using fixed bed models in 1D and 2D
  - Application of the fixed bed model in 3D to simulate a cyclic IBD sub-scale test
  - Optimization of heat transfer for development of a Isothermal Bulk Desiccant (IBD)
  - Studies of the Microlith® Adsorber flow pattern have been used to troubleshoot performance problems and to obtain a successful solution to flow maldistribution
  - Application of the fixed bed model and development of the appropriate vacuum system equations for Vacuum Desorption applications
- Modeling and simulation efforts will continue to maximize the effectiveness of AES ARREM CO_2 Removal system designs